The American Journal of Human Genetics, Volume *106*

Supplemental Data

Neuron-Derived Neurotrophic Factor

Is Mutated in Congenital Hypogonadotropic Hypogonadism

Andrea Messina, Kristiina Pulli, Sara Santini, James Acierno, Johanna Känsäkoski, Daniele Cassatella, Cheng Xu, Filippo Casoni, Samuel A. Malone, Gaetan Ternier, Daniele Conte, Yisrael Sidis, Johanna Tommiska, Kirsi Vaaralahti, Andrew Dwyer, Yoav Gothilf, Giorgio R. Merlo, Federico Santoni, Nicolas J. Niederländer, Paolo Giacobini, Taneli Raivio, and Nelly Pitteloud

Cases Descriptions

Family #1: *NDNF* p.Lys62* (heterozygous)

The Caucasian male proband was born with cryptorchidism and micropenis. He presented at the age 17 years for failure to undergo spontaneous puberty. At that time, he had prepubertal testis (testicular volume <3 ml) with low levels of testosterone and gonadotropins consistent with congenital hypogonadotropic hypogonadism. MRI examination showed a normal pituitary and rudimentary olfactory bulbs, and formal smell testing confirmed anosmia. He exhibited no other CHH-associated phenotypes. He was diagnosed with Kallmann syndrome and testosterone therapy was initiated to develop secondary sexual characteristics. His family history is notable for hyposmia in the father (Cross-Culture Smell ID test [CC-SIT],sit score 8/12), who also carries the heterozygous *NDNF* mutation. The patient's mother and brother had normal sense of smell (mother, CC-SIT score 11/12; brother, CC-SIT score 10/12).

Family #2: *NDNF* Tyr128Thrfs*55 (heterozygous)

The Caucasian male proband was born with bilateral cryptorchidism with subsequent orchidopexy at age 2. He presented at age 13 for failure to undergo spontaneous pubertal development and no growth spurt. On examination he had prepubertal testis (testicular volume 2 ml) with low levels of testosterone and gonadotropins consistent with congenital hypogonadotropic hypogonadism. MRI examination showed bilateral olfactory bulb hypoplasia and a normal pituitary. He exhibited no other CHH-associated phenotypes except for anosmia. He was diagnosed with Kallmann syndrome and started on testosterone to develop secondary sexual characteristics. At age 16.5 years, , he had treatment withdrawal and biochemical testing confirmed persistent hypogonadotropic hypogonadism. Subsequently, he received combined gonadotropin treatment (hCG+FSH) for 2 years and his testicular volume increased to 5ml

under treatment. His parents and his sister self-report both normal smell and reproductive development, however formal smell testing and hormonal investigations were not conducted.

Family #3: *NDNF* p.Trp469* (heterozygous)

The Caucasian female was born at full term without any congenital anomalies. She first presented at age 17 for evaluation of primary amenorrhea. At that time, she exhibited some adrenarche with scant axillary hair, Tanner II pubic hair and Tanner II breast development. She was noted to be anosmic, subsequently confirmed by formal smell test (UPSIT 11/40, <5th percentile). X-rays revealed severely delayed bone age (bone age of 12 years, chronological age of 17 years) and ultrasound showed small ovaries with a small, un-estrogenized uterus. Dynamic testing demonstrated normal anterior pituitary function and serum hormone profiling indicated hypogonadotropic hypogonadism with low serum gonadotropins (LH 1.1 IU/L, FSH 0.6 IU/L) in the setting of undetectable estradiol (<30 pg/mL). The clinical and biochemical picture was consistent with Kallmann syndrome with complete absence of puberty. She was started on estrogen therapy at age 18 which induced breast development, and estro-progestins provided regular withdrawal bleeds.

At age 25 the proband underwent *in vitro* fertilization and gave birth to healthy triplets (one girl and two non-identical twin boys). The proband's daughter is normosmic (UPSIT score 38/40) and her age of menarche was 12 years. This daughter is a non-expressing carrier of the *NDNF* mutation, which is consistent with incomplete penetrance. Clinical and genetic information on the two boys is unavailable. The family history includes delayed puberty in both of the proband's brothers who also harbor the heterozygous *NDNF* mutation. Interestingly, these brothers had an apparently normal initiation of puberty, however did not complete their growth spurt until ages 25 and 28, respectively, raising the question of partial CHH in these individuals. One brother is hyposmic (UPSIT score 28/40, 6th percentile).

The proband and her brothers inherited the mutation from the father who had a low score in the formal smell test (UPSIT score 31/40, 58th percentile), however this is considered normal for his age (>70 years old at time of testing). The proband's mother has a normal sense of smell (UPSIT score 36/40), and has a normal reproductive phenotype (menarche at 14 years old).

Family #4: *NDNF* p.Thr201Ser (heterozygous)

The Caucasian male was born with micropenis and bilateral cryptorchidism for which he underwent orchidopexy at age 4. He then presented at age 16 for failure to undergo spontaneous pubertal development. He was undervirilized with modest axillary hair, eunuchoidal proportions (armspan 178cm, height of 172 cm), and prepubertal testes (1mL bilaterally). Radiologic examination revealed a delayed bone age and hormonal profiling was consistent with CHH. Based on this finding and his anosmia he was diagnosed with Kallmann syndrome and initiated testosterone replacement therapy to induce development of secondary sexual characteristics. His paternal grandfather is anosmic, consistent with familial KS.

Supplementary Figures

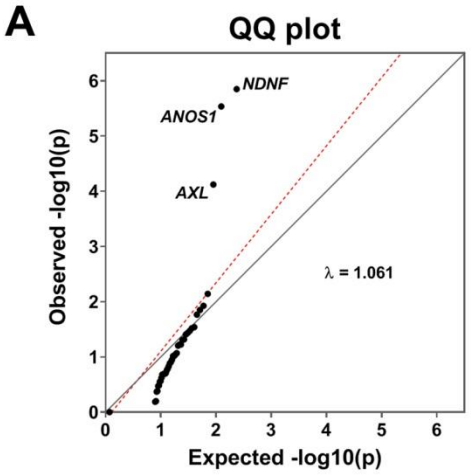

Figure S1. QQ plot illustrating the distribution of observed and expected p-values in the burden analysis of rare PTVs in FN3 genes (CHH patients versus gnomAD control database).

Supplemental Materials and Methods

Subjects, DNA sequencing and bioinformatic analysis

Centre Hospitalier Universitaire Vaudois (CHUV)

A total of 222 CHH unrelated probands (124 KS and 98 nCHH) from primarily European ancestries were included in the study. The diagnosis of CHH was determined via clinical, hormonal and radiologic evaluations as previously described [1; 2]. Additionally, in the presence of hyposmia or anosmia (either self-reported anosmia, or score <5th percentile on formal smell testing, [3; 4] Kallmann syndrome (KS) was diagnosed. When available, family members were recruited for phenotyping and genetic studies.

Whole exome sequencing (WES) was performed by BGI, Inc., Shenzhen, China. Briefly, exonic region capture using Agilent™ V2 or Agilent™ V5 and then enriched *via* library amplification. Exome capture libraries were sequenced on the Illumina™ HiSeq2000™ platform, generating .fastq paired-end files as output. The FASTQ files generated from WES were aligned in-house to the human reference sequence (UCSC GRCh37/hg19 build) using Burrows-Wheeler Aligner (BWA) algorithm, and variants were called with Genome Analysis Toolkit (GATK) [5].

Helsinki University Hospital (HUH)

Genomic DNA samples from 18 male unrelated CHH probands (15 with KS and 3 with nCHH) [6; 7] as well as one KS brother were investigated with WES. WES was provided by three different vendors (Finnish Institute of Molecular Medicine, seven samples; Axeq/Macrogen (South Korea), nine samples) as previously described [8; 9] and two samples were analyzed by Knome Inc. (US). The raw sequence data from the three WES providers were aligned in-house to the human reference sequence (UCSC GRCh37/hg19 build) using Burrows-Wheeler Aligner (BWA) algorithm. Variants were called with Genome Analysis Toolkit (GATK) [5], and visualized and analyzed with the program BasePlayer [10] .

Sanger sequencing.

The coding exons and splice junctions (≤15 bp from exon-intron boundaries) DNA sequences of *NDNF* (RefSeq NM_024574) were PCR-amplified from the genomic DNA of CHH patients. PCR products were purified with ExoSAP-IT treatment (Amersham Biosciences, Piscataway, N.J., USA), and bi-directionally sequenced using the ABI BigDyeTerminator Cycle Sequencing Kit (v3.1) and ABI Prism 3730xl DNA Analyzer automated sequencer (Applied Biosystems, Foster City, Calif., USA) by Microsynth AG, Balgach, Switzerland. Sequence variations were found on both DNA strands and were confirmed in a separate PCR. The sequences were aligned and read with Sequencher® 4.9 software (Gene Codes Corporation,

AnnArbor, Mich., USA) or Chromas Lite 2.01 (Technelysium, Australia). All primer sequences and PCR conditions are indicated below.

NDNF_Ex2F	TGTGACTTGCCTGAGTGTCTGC
NDNF_Ex2R	GCAAGCATTGCCTCCTACACG
NDNF_Ex3F	CAGATCCTTGGGGCTGTTGG
NDNF_Ex3R	TGATGCCACCCTCCCACTTC
NDNF_Ex4aF	TTGGCAAGCCACAGTGTATGCC
NDNF_Ex4aR	AAGCGGTGCTCATGTTGCTG
NDNF_Ex4bF	ACGCAGTTTCCAGGCAAAGC
NDNF_Ex4bR	CACGGTGGCTGAGGAACAGG
NDNF_Ex4cTF	TTCACTCTTGTCTGGATGCTG
NDNF_Ex4cTR	CAGGTCACAACTTCTCTCAACTG

Additional internal primer for sequencing:

NDNF_Ex3intF	CTGGTAAGTCTTGATTGTAAATGTTAG

Bioinformatic analyses.

Variants were annotated using the SnpEff (http://snpeff.sourceforge.net/) and Variant Effect Predictor (VEP) (http://www.ensembl.org/info/docs/tools/vep/index.html; last access, January 2019) tools. In addition to standard annotations, these tools provide data regarding multiple protein prediction models (PolyPhen-2 [11], SIFT [12], Mutation Taster [13], LRT, FATHMM). Genotypes were filtered to include only variants that had minor allele frequencies (MAF) of <1.0% in European controls (gnomAD, all populations).

Subjects found to harbor mutations in FN3-superfamily genes were screened by whole exome or genome sequencing for known loci underlying CHH (see list below).

Gene	OMIM #	OMIM phenotype	Report of oligogenicity
CCDC141	616031	Hypogonadotropic hypogonadism	-
CHD7	608892	CHARGE syndrome; Hypogonadotropic hypogonadism	Yes
DCC	120470	Mirror movements and/or agenesis of corpus callosum; Familial horizontal gaze palsy with progressive scoliosis (AR); Hypogonadotropic hypogonadism	-
DMXL2	612186	Polyendocrine-polyneuropathy syndrome; Autosomal dominant deafness 71	-
DUSP6	602748	Hypogonadotropic hypogonadism	-
FEZF1	613301	Hypogonadotropic hypogonadism	Yes
FGF17	603725	Hypogonadotropic hypogonadism	Yes
FGF8	600483	Hypogonadotropic hypogonadism	Yes
FGFR1	136350	Hypogonadotropic hypogonadism; Hartsfield syndrome; Jackson-Weiss syndrome; Osteoglophonic dysplasia; Pfeiffer syndrome; Trigonocephaly 1	Yes
FLRT3	604808	Hypogonadotropic hypogonadism	-
FSHB	136530	Hypogonadotropic hypogonadism	-
GNRH1	152760	Hypogonadotropic hypogonadism	Yes
GNRHR	138850	Hypogonadotropic hypogonadism	Yes
HS6ST1	604846	Hypogonadotropic hypogonadism	Yes
IGSF10	617351	Delayed puberty; Hypogonadotropic hypogonadism (?)	-
IL17RD	606807	Hypogonadotropic hypogonadism	-
KAL1	300836	Hypogonadotropic hypogonadism	Yes
KISS1	603286	Hypogonadotropic hypogonadism	Yes
KISS1R	604161	Hypogonadotropic hypogonadism; Precocious puberty (AD)	Yes
KLB	611135	Hypogonadotropic hypogonadism	-
LEP	164160	Obesity, morbid, due to leptin deficiency	Yes
LEPR	601007	Obesity, morbid, due to leptin receptor deficiency	Yes
LHB	152780	Hypogonadotropic hypogonadism	-
NR0B1	300473	Adrenal hypoplasia, congenital	-
NSMF	608137	Hypogonadotropic hypogonadism	Yes
NTN1	601614	Hypogonadotropic hypogonadism	-

OTUD4	611744	Hypogonadotropic hypogonadism	-
PCSK1	162150	Obesity with impaired prohormone processing	Yes
PLXNA1	601055	Hypogonadotropic hypogonadism	-
PNPLA6	603197	Boucher-Neuhauser syndrome; Oliver-McFarlane syndrome; Spastic paraplegia 39; Laurence-Moon syndrome	-
POLR3A	614258	Leukodystrophy hypomyelinating 7 with or without oligodontia and/or hypogonadotropic hypogonadism	-
POLR3B	614366	Leukodystrophy hypomyelinating 8 with or without oligodontia and/or hypogonadotropic hypogonadism	-
PROK2	607002	Hypogonadotropic hypogonadism	Yes
PROKR2	607123	Hypogonadotropic hypogonadism	Yes
RNF216	609948	Cerebellar ataxia and hypogonadotropic hypogonadism	-
SEMA3A	603961	Hypogonadotropic hypogonadism	Yes
SEMA3E	608166	CHARGE syndrome (possible) Hypogonadotropic hypogonadism	-
SMCHD1	614982	Bosma arhinia microphthalmia syndrome; Hypogonadotropic hypogonadism	-
SOX10	602229	PCWH syndrome; Waardenburg syndrome type 2E; Waardenburg syndrome type 4C; Hypogonadotropic hypogonadism	Yes
SOX2	184429	Syndromic microphthalmia 3 Optic nerve hypoplasia and CNS abnormalities Hypogonadotropic hypogonadism	-
SPRY4	607894	Hypogonadotropic hypogonadism	-
STUB1	607207	Spinocerebellar ataxia 16 Hypogonadotropic hypogonadism	-
TAC3	162330	Hypogonadotropic hypogonadism	Yes
TACR3	162332	Hypogonadotropic hypogonadism	Yes
TUBB3	602661	TUBB3 E410K syndrome with hypogonadotropic hypogonadism	-
WDR11	606417	Hypogonadotropic hypogonadism	Yes
AXL	109135	Hypogonadotropic hypogonadism	-

***In vitro* analysis of NDNF mutants**

Western blot.

Sub-confluent COS7 cells in 24-well plates were transiently transfected with 5 ng or 100 ng of flag-tagged WT or mutant NDNF for analysis of cell lysate and secreted protein levels respectively, using FuGene HD reagent (Roche Diagnostics). Following a 16 h incubation in a full growth medium, the medium was changed to a reduced serum medium (OptiMEM, Life Technology) and the cells were incubated for an additional 24 h. Equal amounts of WT and mutant cleared lysate (5-10 μg of total protein) and 20 ul of cleared conditioned medium were resolved on NuPAGE 10% Bis-Tris gels (Life Technologies) under reducing conditions and then subjected to Western blot analysis using an anti-flag primary antibody (M2 clone, Sigma-Aldrich) and goat anti-mouse horseradish peroxidase-conjugated secondary antibody (Upstate Biotechnology). Blots were stripped using Restore Western Blot Stripping Buffer (Pierce) and re-probed with horseradish peroxidase-conjugated anti-β-actin antibody (Abcam, Cambridge, MA). Flag-NDNF and β-actin immunoreactivity were quantified by densitometry (ImagJ software). Specific NDNF expression levels were normalized to the expression levels of β-actin and reported as a ratio to WT. For analysis of conditioned medium experiments, we measured the NDNF migrating band at an expected molecular weight (Thr201Ser, ~75 kD; Trp463* ~60kD). Experiments were repeated 5 times, and protein expression levels were compared between each mutant and WT protein using Student's t-test. Data are presented as mean ± SEM.

Cell-surface expression.

Sub-confluent COS7 cells were transfected with WT or mutant NDNF plasmids. After 24 h the cells were rinsed and incubated at room temperature for 3-4 h in binding buffer (50 mM Tris-HCl, 100 mM NaCl, 5 mM KCl, 2 mM $CaCl_2$, 5% heat-inactivated horse serum, 0.5% fetal bovine serum, pH 7.7) containing anti-FLAG antibody (1:1500, M2 clone, Sigma-Aldrich). Cells were then rinsed and incubated at room

temperature for 2 h in binding buffer containing [^{125}I]-rabbit anti-mouse IgG (300,000 cpm/well; PerkinElmer), prior to being lysed in 1 N NaOH. The radioactivity in the lysates was measured via gamma-counter, and experiments were performed in quadruplicate. Results were expressed as percent WT, and the mean specific expression levels of WT and mutant NDNF from 4 independent experiments were compared using ANOVA followed by Dunnett's correction for multiple comparisons.

Reporter gene assay.

To detect activation of the PLCγ/Ca^{+2} cascade downstream of FGF8/FGFR1 we used the nuclear factor of activated T-cells (NFAT)-luciferase reporter (addgene plasmid 10959; Ichida, M. and Finkel, T. 2001 *J Biol Chem*, 276; [14; 15]. COS7 cells were transiently transfected with 75ng NFAT-Luc reporter together with 5ng FGFR1, 10ng WT or mutant NDNF expression plasmids, and 110ng pCDNA3.1 empty vector using FuGENE HD reagent (Promega). Following a 16h incubation in full growth medium, cells were starved in serum free medium for 8h and then stimulated overnight with increasing doses (0-50 nM) of FGF8 (provided by Dr. M. Mohammadi). Assays were preformed in triplicate and repeated at least 3 times. Reporter activation levels of WT and mutant NDNF from each experiment were expressed as a percent of the maximal FGF8 dose response obtained in the absence of NDNF, and the mean values from 3 independent experiments were fitted using a three-parameter sigmoidal curve (Prism6, GraphPad Software). Response at the highest dose of mutant NDNF was compared to that of WT using ANOVA followed by Dunnett's correction for multiple comparisons.

Production and purification of human recombinant NDNF

Full-length untagged 568 aa recombinant human NDNF protein (Uniprot Q8TB73) was produced using the QMCF stable episomal expression system following cDNA codon optimization in CHO cells by Icosagen,

Estonia. Purification of secreted recombinant NDNF from CHO culture medium was performed by denaturation with 3M urea followed by HiTrap SP HP cation exchange chromatography. Protein was eluted with 20 mM Na-phosphate pH 7.0 with 2 M NaCl. Eluted protein was further purified by gel filtration with Superdex 200 Increase 10/300 column followed by buffer exchange into the PBS (pH 7,4), 0.7M NaCl. Product was concentrated to 1 mg/ml by Amicon concentrator, and protein concentration was verified by Nanodrop (Ext coef. 46.6).

In vivo zebrafish model

Zebrafish strains and treatments.

Morpholinos sequences for NDNF (wu:fb16h09):

zFB16-SS	CTGGCTCACCTAAGACACAGGAAAC
zFB16-ATG	ATAACATCCACACCTCCACGTCATC

Control MO sequence:

5' TCGTGGCCATCAACTCGAACA 3'

NDNF expression studies

Fluorescence-activated cell sorting and gene expression analysis.

Embryos were harvested at E14.5 and E18.5 from timed-pregnant GnRH-GFP mice anesthetized with an i.p. injection of 100 mg/kg of ketamine-HCl and sacrificed by cervical dislocation. Microdissected tissues were enzymatically dissociated using the Papain Dissociation System (Worthington, Lakewood, NJ) to obtain single-cell suspensions as previously described [16]. After dissociation, the cells were physically purified using a FACSAria III (Beckman Coulter) flow cytometer equipped with FACSDiva software (BD

Biosciences). The sort decision was based on measurements of GFP fluorescence (excitation: 488nm, 50 mW; detection: GFP bandpass 530/30 nm, autofluorescence bandpass 695/40nm) by comparing cell suspensions from GnRH-GFP and wild-type animals. For each animal, 500 GFP-positive cells and 500 GFP-negative cells were sorted directly into 8µl of extraction buffer: 0.1% Triton X-100 (Sigma-Aldrich) and 0.4 U/µl RNaseOUT™ (Life Technologies). Captured cells were used to synthesize first-strand cDNA using the SuperScript III First-Strand Synthesis System for reverse transcription (RT)-PCR (Invitrogen) following the manufacturer's instructions. Controls without reverse transcriptase were performed to demonstrate the absence of contaminating genomic DNA. We used SuperScript® III Reverse Transcriptase (Life Technologies) and a linear preamplification step was performed using the TaqMan® PreAmp Master Mix Kit protocol (Applied Biosystems). Real-time PCR was carried out on Applied Biosystems 7900HT Fast Real-Time PCR System using exon-boundary-specific TaqMan® Gene Expression Assays (Applied Biosystems): *Gnrh1* (Mm01315605_m1), *NDNF* (Mm00549567_m1), *Actin* (Mm00607939_s1), *Rn18S* (Mm04277571_s1). Quantitative real-time PCR was performed using TaqMan Low-Density Arrays (Applied BioSystems) on an Applied BioSystems 7900HT thermocycler using the manufacturer's recommended cycling conditions. Gene expression data were analyzed using SDS 2.4.1 and Data Assist 3.0.1 software (Applied BioSystems). Data were compared by one-way ANOVA for multiple comparisons followed by Tukey's least significant difference post hoc test. The significance level was set at $p < 0.05$ in all cases. Data are represented by means ± SEM.

Ndnf knock-out mice

Genotyping of the mice was performed with DNA isolated from ear samples or from decapitated mouse embryos with Macherey-Nagel NucleoSpin Tissue kit according to manufacturer's instructions.

Genotyping was performed by PCR and agarose gel electrophoresis. Primers used in genotyping are shown in the table below.

Reaction	Primer name	Primer sequence	Product size
PCR to detect mutant allele	KO_Ndnf_Fw	5' ACAATTGTTCACTCTGCTCACCAG 3'	300 bp
	KO_Ndnf_Rv	5' TCGTGGTATCGTTATGCGCC 3'	
PCR to detect wild type allele	WT_Ndnf_Fw	5' GACTTCCTTTGTACTGTCTTGGG 3'	675 bp
	WT_Ndnf_Rv	5' TGTGCCCTCTACATCAGTCA 3'	

iDISCO whole-mount staining

Experiments were performed as previously described (Renier et al., Cell 2014) and detailed below.

Sample pre-treatment with methanol

Samples were washed in PBS (twice for 1h), followed by 50% methanol in PBS (once for 1h), 80% methanol (once for 1h) and 100% methanol (twice for 1h). Next, samples were bleached in 5% H_2O_2 in 20% DMSO/methanol (2ml 30% H_2O_2/2ml DMSO/8ml methanol, ice cold) at 4°C overnight. Next, samples were washed in methanol (twice for 1h), in 20% DMSO/methanol (twice for 1h), 80% methanol (once for 1h), 50% methanol (once for 1h), PBS (twice for 1h), and finally, PBS/0.2% TritonX-100 (twice for 1h) before proceeding to the staining procedures.

Samples were incubated at 37°C on an adjustable rotator in 10 ml of a blocking solution (PBSGNaT) of 1X PBS containing 0.2% gelatin (Sigma), 0.5% Triton X-100 (Sigma-Aldrich) and 0.01% NaAzide for 3 nights. Samples were transferred to 10 ml of PBSGNaT containing primary antibodies (see *GnRH cell counting* for details) and placed at 37°C in rotation for 7 days. This was followed by six washes of 30min in PBSGT at RT and a final wash in PBSGT overnight at 4°C. Next, samples were incubated in secondary antibodies

(1:400, Alexa 568, Alexa 647) diluted in 10 ml PBSGNaT for 2 days at 37°C in a rotating tube. After six 30-min washes in PBS at room temperature, the samples were stored in PBS at 4°C in the dark until clearing.

Tissue clearing

All incubation steps were performed at RT in a fume hood on a tube rotator at 14 rpm covered with aluminium foil to avoid contact with light. Samples were dehydrated in a graded series (50%, 80%, and 100%) of tetrahydrofurane (THF; anhydrous, containing 250 ppm butylated hydroxytoluene inhibitor, Sigma-Aldrich) diluted in H2O as follow: 1) 50% THF overnight at RT; 2) 80% THF 1h at RT; 3) 100% THF 1h30 at RT; 4) 100% THF 1h30 at RT. This was followed by a delipidation step of 30-40 min in 100 % dichloromethane (DCM; Sigma-Aldrich). Samples were cleared in dibenzylether (DBE; Sigma-Aldrich) for 2h at RT on constant agitation and in the dark. Finally, samples were moved into fresh DBE and stored in glass tubes in the dark and at RT until imaging. We could image samples, as described below, without any significant fluorescence loss for up to 6 months.

Imaging

3D imaging was performed as previously described (Belle et al., 2014) using an ultramicroscope (LaVisionBioTec) with ImspectorPro software (LaVisionBioTec). The light sheet was generated by a laser (wavelength 488 or 561 nm, Coherent Sapphire Laser, LaVisionBioTec) and two cylindrical lenses. A binocular stereomicroscope (MXV10, Olympus) with a 2× and 4x objective (MVPLAPO, Olympus) was used at different magnifications (1.6×, 4×, 5×, and 6.3×). Samples were placed in an imaging reservoir made of 100% quartz (LaVisionBioTec) filled with DBE and illuminated from the side by the laser light. A PCO Edge SCMOS CCD camera (2560 × 2160 pixel size, LaVisionBioTec) was used to acquire images. The step size between each image was fixed at 2 µm.

Image analysis

For confocal observations and analyses, an inverted laser scanning Axio observer microscope (LSM 710, Zeiss, Oberkochen, Germany) with EC Plan NeoFluor 10×/0.3 NA, 20×/0.5 NA and 40×/1.3 NA (Zeiss, Oberkochen, Germany) objectives were used (Imaging Core Facility of IFR114 of the University of Lille, France).

Images, 3D volume, and movies were generated using Imaris x64 software (version 7.6.1, Bitplane). Stack images were first converted to imaris file (.ims) using ImarisFileConverter and 3D recontruction was performed using "volume rendering". Optical slices of samples were obtained using the "orthoslicer" tools. The surface of the samples was created using the "surface" tool by creating a mask around each volume. The peripherin-positive fibers and GnRH neurons were segmented to allow easier visualization and comparison between samples. 3D pictures were generated using the "snapshot" tool. ImageJ (National Institute of Health, Bethesda, USA) and Photoshop CS6 (Adobe Systems, San Jose, CA, USA) were used to process, adjust and merge the photomontages. Figures were prepared using Adobe Photoshop and Abode Illustrator CS6.

Supplemental references

1. Pitteloud, N., Hayes, F.J., Boepple, P.A., DeCruz, S., Seminara, S.B., MacLaughlin, D.T., and Crowley, W.F., Jr. (2002). The role of prior pubertal development, biochemical markers of testicular maturation, and genetics in elucidating the phenotypic heterogeneity of idiopathic hypogonadotropic hypogonadism. J Clin Endocrinol Metab 87, 152-160.
2. Pitteloud, N., Hayes, F.J., Dwyer, A., Boepple, P.A., Lee, H., and Crowley, W.F., Jr. (2002). Predictors of outcome of long-term GnRH therapy in men with idiopathic hypogonadotropic hypogonadism. J Clin Endocrinol Metab 87, 4128-4136.
3. Doty, R.L., Shaman, P., Kimmelman, C.P., and Dann, M.S. (1984). University of Pennsylvania Smell Identification Test: a rapid quantitative olfactory function test for the clinic. Laryngoscope 94, 176-178.
4. Doty, R.L., Marcus, A., and Lee, W.W. (1996). Development of the 12-item Cross-Cultural Smell Identification Test (CC-SIT). Laryngoscope 106, 353-356.
5. McKenna, A., Hanna, M., Banks, E., Sivachenko, A., Cibulskis, K., Kernytsky, A., Garimella, K., Altshuler, D., Gabriel, S., Daly, M., et al. (2010). The Genome Analysis Toolkit: a MapReduce framework for analyzing next-generation DNA sequencing data. Genome Res 20, 1297-1303.
6. Laitinen, E.M., Vaaralahti, K., Tommiska, J., Eklund, E., Tervaniemi, M., Valanne, L., and Raivio, T. (2011). Incidence, phenotypic features and molecular genetics of Kallmann syndrome in Finland. Orphanet J Rare Dis 6, 41.
7. Laitinen, E.M., Tommiska, J., Sane, T., Vaaralahti, K., Toppari, J., and Raivio, T. (2012). Reversible congenital hypogonadotropic hypogonadism in patients with CHD7, FGFR1 or GNRHR mutations. PloS one 7, e39450.
8. Sulonen, A.M., Ellonen, P., Almusa, H., Lepisto, M., Eldfors, S., Hannula, S., Miettinen, T., Tyynismaa, H., Salo, P., Heckman, C., et al. (2011). Comparison of solution-based exome capture methods for next generation sequencing. Genome Biol 12, R94.
9. Palmio, J., Evila, A., Chapon, F., Tasca, G., Xiang, F., Bradvik, B., Eymard, B., Echaniz-Laguna, A., Laporte, J., Karppa, M., et al. (2014). Hereditary myopathy with early respiratory failure: occurrence in various populations. J Neurol Neurosurg Psychiatry 85, 345-353.
10. Katainen, R., Donner, I., Cajuso, T., Kaasinen, E., Palin, K., Makinen, V., Aaltonen, L.A., and Pitkanen, E. (2018). Discovery of potential causative mutations in human coding and noncoding genome with the interactive software BasePlayer. Nat Protoc 13, 2580-2600.
11. Adzhubei, I.A., Schmidt, S., Peshkin, L., Ramensky, V.E., Gerasimova, A., Bork, P., Kondrashov, A.S., and Sunyaev, S.R. (2010). A method and server for predicting damaging missense mutations. Nature methods 7, 248-249.
12. Kumar, P., Henikoff, S., and Ng, P.C. (2009). Predicting the effects of coding non-synonymous variants on protein function using the SIFT algorithm. Nature protocols 4, 1073-1081.
13. Schwarz, J.M., Rodelsperger, C., Schuelke, M., and Seelow, D. (2010). MutationTaster evaluates disease-causing potential of sequence alterations. Nature methods 7, 575-576.
14. Ichida, M., and Finkel, T. (2001). Ras regulates NFAT3 activity in cardiac myocytes. J Biol Chem 276, 3524-3530.
15. Crabtree, G.R., and Olson, E.N. (2002). NFAT signaling: choreographing the social lives of cells. Cell 109 Suppl, S67-79.
16. Giacobini, P., Parkash, J., Campagne, C., Messina, A., Casoni, F., Vanacker, C., Langlet, F., Hobo, B., Cagnoni, G., Gallet, S., et al. (2014). Brain Endothelial Cells Control Fertility through Ovarian-Steroid-Dependent Release of Semaphorin 3A. PLoS biology 12, e1001808.